Available online at www.sciencedirect.com
ScienceDirect
Journal of the European Ceramic Society 28 (2008) 2025–2032
www.elsevier.com/locate/jeurceramsoc

A stabilization mechanism for the perovskite $La_{2/3}TiO_3$ compound with Fe_2O_3: A structural and electrical investigation

Srečo Davor Škapin [a], Andrijana Sever Škapin [b], Danilo Suvorov [a], Miran Gaberšček [c,*]

[a] *Jožef Stefan Institute, Jamova 39, SI-1000 Ljubljana, Slovenia*
[b] *Slovenian National Building and Civil Engineering Institute, Dimičeva 12, SI-1000 Ljubljana, Slovenia*
[c] *National Institute of Chemistry, Laboratory for Materials Electrochemistry, POB 660, Hajdrihova 19, SI-1000 Ljubljana, Slovenia*

Received 11 July 2007; received in revised form 12 December 2007; accepted 20 December 2007
Available online 3 March 2008

Abstract

We have stabilized the perovskite $La_{2/3}TiO_3$ by adding $LaFeO_3$ and shown that in general the stabilization mechanism for the $(1-x)La_{2/3}TiO_{3-x}LaFeO_3$ mixture involves the formation of a solid solution for compositions with $x \geq 0.04$. The crystal structure of the solid solution transforms from orthorhombic to tetragonal at $x = 0.2$, becomes cubic in the range $0.3 < x < 0.8$, and transforms again into orthorhombic (typical for pure $LaFeO_3$) for values greater than 0.8. Detailed impedance-spectroscopy measurements for various compositions and conditions showed that the limiting step in the conduction mechanism was conduction across the grain boundaries. In the concentration range $0.04 < x < 0.25$ the room temperature conductivity increases up to $0.0017\,S\,cm^{-1}$, after which it decreases again. Part of the initial increase is probably due to the formation of free electrons in accordance with $(Fe_{Ti})' \rightarrow (Fe_{Ti})^x + n'$. Other defect-formation mechanisms are also discussed, but are ruled out for a variety of reasons. Another interesting phenomenon that also affected the average conductivity was identified, i.e., the variation of the average particle size with composition.

Keywords: Perovskites; Solid solution; Defects; Electrical conductivity; Fuel cells; $La_{2/3}TiO_3$

1. Introduction

Ceramics based on the perovskite $La_{2/3}TiO_3$ compound are promising candidates for the manufacture of high-frequency components, e.g., resonators and oscillators. It is well known from previous studies that under normal atmospheric conditions (containing oxygen) the perovskite $La_{2/3}TiO_3$ compound does not form due to the formation of vacancies at the La-sites in the crystal structure.[1] Thus, heating a La_2O_3/TiO_2 mixture in the molar ratio 1:3 up to ≈1455 °C in air results in the formation of two phases: $La_4Ti_9O_{24}$ and $La_2Ti_2O_7$.[2,3] The preparation of the $La_{2/3}TiO_3$ compound (with the general formula $La_{2/3}(V_{La})_{1/3}TiO_3$) is possible via three routes: by heating the oxides in a slightly reducing atmosphere,[1] by stabilizing the system with the addition of other perovskites, e.g., $LaAlO_3$,[4] $SrTiO_3$[5] and $PbTiO_3$,[6] or by the incorporation of alkaline ions into its crystal structure.[7]

In our previous investigation[4] we proved that a small addition of $LaAlO_3$ (4 mol%) to $La_{2/3}TiO_3$ completely stabilized the perovskite $La_{2/3}TiO_3$ structure with doubled unit cell. Furthermore, we showed that the stabilized $La_{2/3}TiO_3$ and $LaAlO_3$ formed a solid solution in the whole concentration range. In this solid solution, which can be described by a general formula $La_{(2+x)/3}Ti_{(1-x)}Al_xO_3$, the Ti ions on B sites are progressively substituted by Al ions as the amount of added $LaAlO_3$ is increased. We also found that by varying the $La_{2/3}TiO_3/LaAlO_3$ ratio several inherent materials properties, especially those interesting for potential microwave application, were changed continuously and in relatively wide ranges. For example, the permittivity (ε) could be varied from 40 to 75, the quality factor Qxf_r was increased from 12,000 GHz to 45,000 GHz and the temperature coefficient of resonant frequency τ_f could have values from 120 ppm/K to −25 ppm/K.[8]

Motivated by the wide-range tunability of the properties of $La_{(2+x)/3}Ti_{(1-x)}Al_xO_3$ solid solutions, we wondered what

* Corresponding author. Tel.: +386 61 1760 320; fax: +386 61 4760 300.
E-mail address: miran.gaberscek@ki.si (M. Gaberšček).

0955-2219/$ – see front matter © 2008 Elsevier Ltd. All rights reserved.
doi:10.1016/j.jeurceramsoc.2007.12.036

happened if Al was replaced with an aliovalent element. We speculated that in such a case, the solid solution could also show tunable conductivity—owing to creation of defect structures, such as oxygen vacancies, free electrons/holes, etc. as a function of composition. We further assumed that a good candidate for such a purpose would be iron in the form of $LaFeO_3$ which itself exhibits a considerable p-type electrical semiconductivity (1.5×10^{-6} S cm^{-1})[9,10] and, as such, has been found interesting for applications in SOFCs, as catalysts and for gas sensors.[11–13] We hoped that a solid solution prepared by combining $LaFeO_3$ with $La_{2/3}TiO_3$ would show an even higher conductivity. $LaFeO_3$ is also a good choice from the structural point of view: it crystallizes in the orthorhombic perovskite structure with the lattice parameters $a = 5.553$ Å, $b = 5.563$ Å and $c = 7.867$ Å.[14]

There is a significant amount of data in the literature on the conductivity mechanisms in pure $LaFeO_3$. Goodenough[15] found that the basic mechanism involved a small-polaron hopping conduction that occurred *via* the d-electron band of Fe ions, which is characteristic for the octahedral coordination of Fe^{3+} with six O^{2-} neighbours. On the other hand, the ionic contribution to the total conductivity in orthoferrites was assumed to be small and could be neglected at temperatures up to about 1000 °C.[16] Further investigations into the conduction processes confirmed the previous assumptions that the major defects present in $LaFeO_3$ are p (Fe^{4+}), *n* (Fe^{2+}), $(V_{La})'''$ and $(V_O)^{\bullet\bullet}$, so that the compound could be represented by the general formula $La_{1-x}FeO_{3-z}$.[17] It was also suggested that the lanthanum vacancies may have been introduced during the sample preparation and caused a deviation from the stoichiometric ratio La/Fe = 1. Thus, the prevailing type of electrical conductivity, i.e., p- or n-type, depends on $p_{(O2)}$ and the La/Fe ratio.[17]

Based on the above considerations, the main purpose of the present investigation is to find whether the $La_{2/3}TiO_3$ structure can be stabilized using $LaFeO_3$. In particular, we are interested if such a stabilization can occur *via* the same mechanism as in the case of $LaAlO_3$,[4] that is, by formation of a solid solution. We also expect that, unlike in the aforementioned case, the stabilized structure (e.g., the solid solution) will exhibit a significant conductivity, possibly dependent on composition but, in any case, higher than that found for pure $LaFeO_3$. Using a detailed impedance spectroscopy analysis in conjunction with structural and microstructural observations, we also intend to determine the conduction mechanism in the prepared samples.

2. Experimental

All the samples were prepared using a conventional solid-state reaction technique and high-purity La_2O_3, TiO_2 and Fe_2O_3. Since La_2O_3 has a strong tendency to form hydroxide and carbonate with moisture and CO_2 from the air, the oxide was routinely checked prior to weighing with ignition tests at 1300 °C.

The weighed oxides in the proper ratio according to the nominal formula $(1-x)La_{2/3}TiO_3$–$xLaFeO_3$, where x was varied between 0 and 1 were homogenized in a YTZ ball mill for 0.5 h with ethanol. The dried mixtures were uniaxially pressed into disks and fired in a tube furnace at 1400 °C for 20 h. After sintering, the samples were slowly cooled in the furnace. In the second series of experiments the samples were air quenched after the first sintering, and after crushing and homogenizing they were again thermally treated at the same temperature. Like in the previous case, the samples were slowly cooled in the furnace.

For the impedance-spectroscopy measurements the disks were cut into 2–3-mm-thick slices, with some slices being slightly thinner or thicker (see Fig. 6). Thin Au contacts were sputtered on both sides of the disks using a Balzers Sputter Coater 050.

The samples were analyzed using X-ray diffractometry (XRD) (Endeavor D4, Bruker AXS). Polished and thermally etched cross-sections were examined using a scanning electron microscope (SEM, Jeol JXA 840A) equipped with an energy-dispersive spectrometer (EDXS, Tracor Northern, NORAN, Series II).

Impedance spectra were measured in the range 1 MHz to 20 Hz using a Hewlett Packard 4284a Precision LCR Meter. The measurement device was connected to a laboratory-designed gas-tight quartz tube equipped with four appropriately shielded electrical contacts. The measurements were made in an atmosphere of air or argon. For the activation energy measurements, the quartz tube was inserted into a furnace. The temperature was typically varied between 25 °C and 330 °C.

3. Results and discussion

3.1. Stabilization of the $La_{2/3}TiO_3$ perovskite structure

Fig. 1 presents micrographs of four samples containing different amounts of $LaFeO_3$ in the starting composition. Using the $(1-x)\ La_{2/3}TiO_3 - xLaFeO_3$ notation, these samples correspond to the following stoichiometries: (a) $x = 0$, (b) $x = 0.01$, (c) $x = 0.02$ and (d) $x = 0.04$. The pure La_2O_3:3TiO_2 composition ($x = 0$) shows the presence of $La_2Ti_2O_7$ and $La_4Ti_9O_{24}$ phases, in accordance with the La_2O_3–TiO_2 phase diagram.[2,3] However, even the addition of 1 mol% of $LaFeO_3$ ($x = 0.01$) produces a partial stabilization of perovskite $La_{2/3}TiO_3$, as can be seen in Fig. 1b. At $x = 0.02$ (Fig. 1c) a higher proportion of the perovskite compound is formed, while at $x = 0.04$ a single-phase microstructure is obtained (Fig. 1d). With a further increase in $LaFeO_3$ content ($0.04 \leq x \leq 1$), the stabilized $La_{2/3}TiO_3$ compound with $x = 0.04$ forms a solid solution with $LaFeO_3$. Similar behavior was observed in the system with $LaAlO_3$,[4] but not in the system with $LaGaO_3$, where the stability range of the solid solution only extended within $0.06 \leq x \leq 0.12$.[18]

The X-ray diffraction analysis of the same set of four samples confirms the findings from the microstructural studies (Fig. 2), and further reveals that the stabilized $La_{2/3}TiO_3$ perovskite has a doubled unit cell, as demonstrated by the superstructure reflections (Fig. 2, pattern (d)).

The stabilization mechanism of the perovskite $La_{2/3}TiO_3$ during high-temperature formation can be described as follows:

$$(1-x)La_{2/3}V_{1/3}TiO_3 + xLaFeO_3 \rightarrow (La_{(2+x)/3}V_{(1-x)/3})(Ti_{(1-x)}Fe_x)O_3 \quad (1)$$

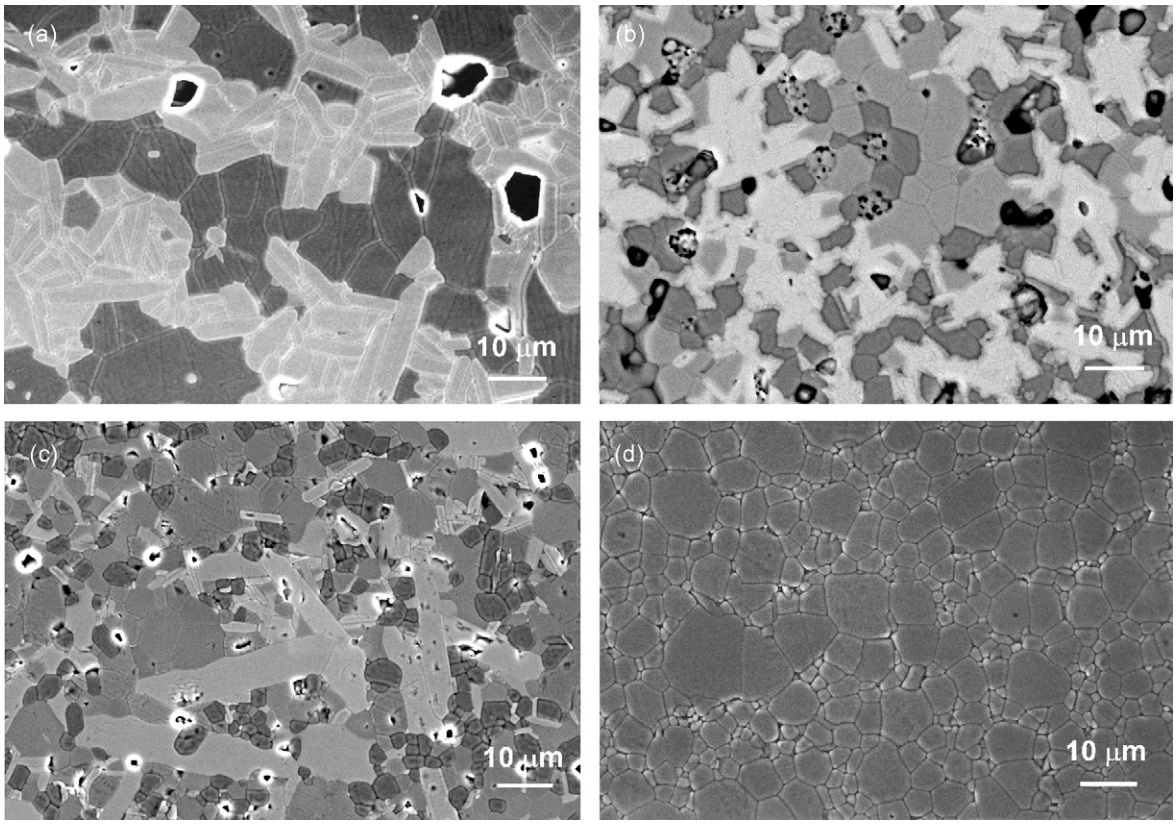

Fig. 1. SEM micrographs of $(1-x)$ $La_{2/3}TiO_{3-x}LaFeO_3$ compositions: (a) $x=0$, (b) $x=0.01$, (c) $x=0.02$ and (d) $x=0.04$ (bright phase: $La_2Ti_2O_7$, gray phase: $La_{2/3}TiO_3$, dark phase: $La_4Ti_9O_{24}$).

We can suppose that the Fe occupies the Ti sites homogeneously and that the number of vacancies at the La sites decreases with increasing Fe content in the perovskite crystal structure.

3.2. Crystal structure of the solid solution $La_{2/3}TiO_3$–$LaFeO_3$

A detailed inspection of the X-ray pattern in Fig. 2(d) reveals that the profile of the fundamental (2 0 0) peak of the single-phase sample ($x=0.04$) is split into three lines corresponding to (2 0 0), (0 2 0) and (0 0 2) (Fig. 3, pattern (a)).[19] This indicates that the stabilized $La_{2/3}TiO_3$ has an orthorhombic distortion with a double unit cell, similar to the case where the stoichiometric $La_{2/3}TiO_3$ structure was stabilized by the partial reduction of Ti^{4+} to Ti^{3+} (1). With the increasing $LaFeO_3/La_{2/3}TiO_3$ ratio the intensity of the splitting of this line diminishes, as exhibited in patterns (b) and (c) in Fig. 3, which correspond to the compositions $x=0.10$ and $x=0.20$, respectively. We can assume

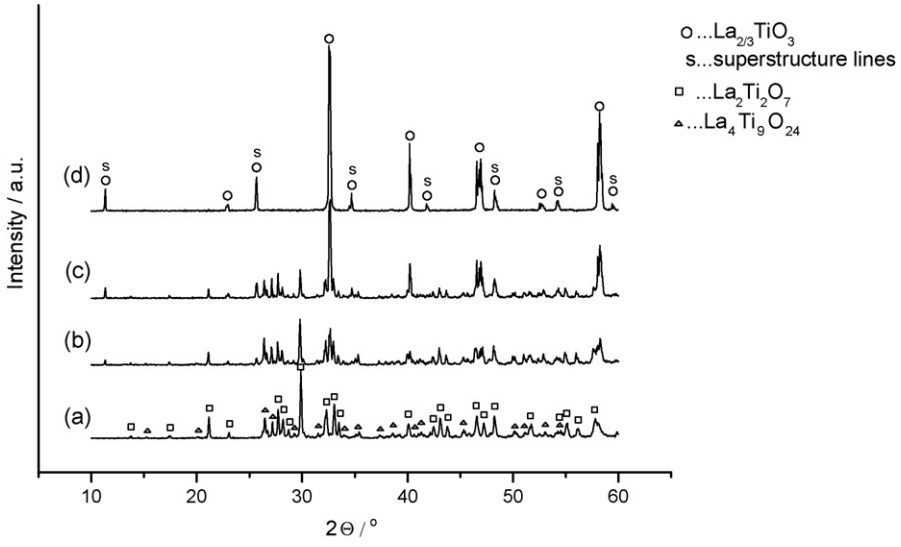

Fig. 2. X-ray powder-diffraction patterns of the $(1-x)$ $La_{2/3}TiO_3$–xLaFeO$_3$ system: (a) $x=0$, (b) $x=0.01$, (c) $x=0.02$ and (d) $x=0.04$.

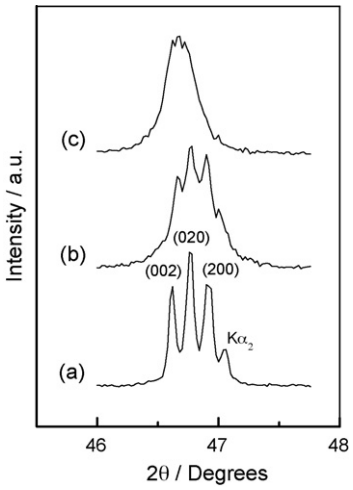

Fig. 3. Part of X-ray powder-diffraction patterns of the $(1-x)$ $La_{2/3}TiO_{3-x}LaFeO_3$ system: (a) $x=0.04$, (b) $x=0.10$ and (c) $x=0.20$.

that the crystal structure of the solid solution transforms from an orthorhombic to a tetragonal structure at $x=0.2$. The tetragonality of the solid solution further decreases with the increasing $LaFeO_3/La_{2/3}TiO_3$ ratio. Thus, at $x=0.3$ the weak, superstructure lines are still present (Fig. 4, pattern (a)), whereas above this composition they disappear (see Fig. 4, pattern (b) corresponding to the cubic structure). The solid solution $La_{2/3}TiO_3$–$LaFeO_3$ remains cubic in the concentration range $x\approx0.3$ to $x\approx0.8$, above which it transforms to the orthorhombic crystal structure typical for pure $LaFeO_3$ (Fig. 4, patterns (c) and (d)).

3.3. Electrical properties as a function of the composition of $La_{2/3}TiO_3$–$LaFeO_3$

The complex-plane impedance spectrum of a $(1-x)$ $La_{2/3}TiO_3$–xLaFeO$_3$ pellet with the composition $x=0.1$ measured at room temperature is shown in Fig. 5a. All the other

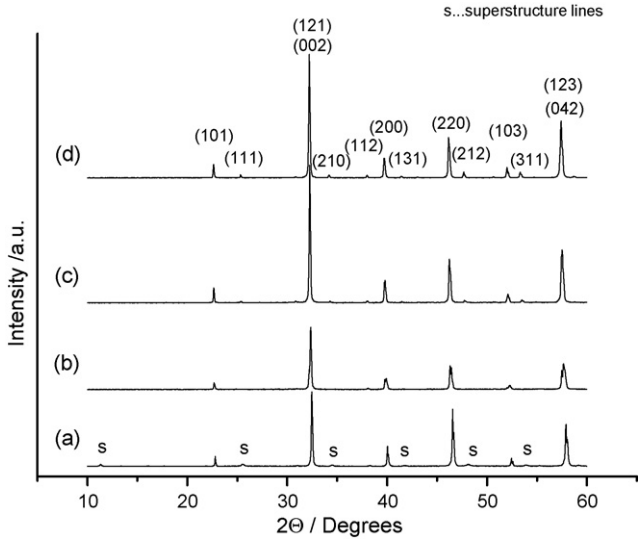

Fig. 4. X-ray powder-diffraction patterns of the $(1-x)$ $La_{2/3}TiO_{3-x}LaFeO_3$ system: (a) $x=0.30$, (b) $x=0.40$, (c) $x=0.80$ and (d) $x=1.0$.

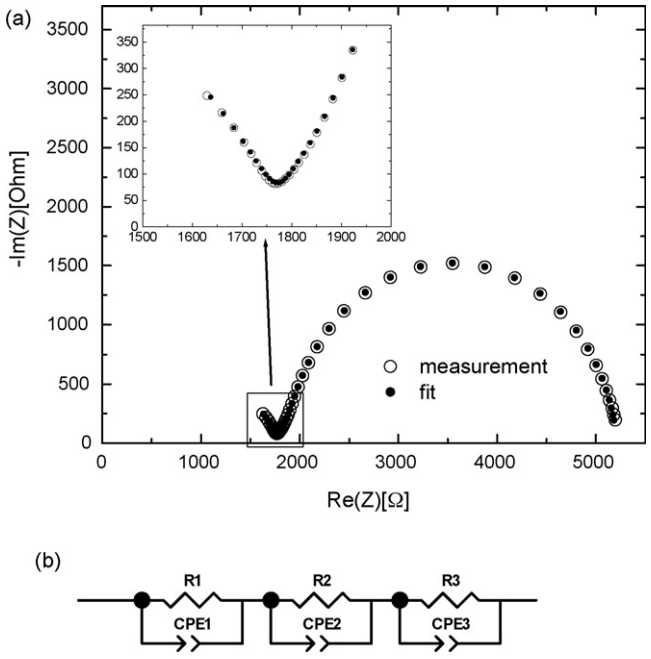

Fig. 5. (a) Measured (open circles) and fitted (full circles) impedance response of a sintered pellet with composition $x=0.1$ at 25 °C. The thickness of the pellet was 2.7 mm and the diameter was 8 mm. The frequency range of measurement was 10^6–20 Hz. (b) The equivalent circuit used to fit the measured response. The meaning of the CPE elements is explained by Eq. (2) (see main text).

samples, for all the temperatures investigated, had the same basic shape in the complex plane. A detailed analysis shows that the high-frequency part can be quite satisfactorily fitted with one resistor (R) in parallel with a constant phase element (CPE), while the low-frequency arc should be fitted with at least two such terms, i.e., what appears as a single arc is, in fact, at least two closely coupled arcs. Here, the impedance response of the CPE is defined as:

$$Z_{CPE}=\frac{1}{(i\omega)^P C} \tag{2}$$

where $i=\sqrt{-1}$, ω is the angular frequency of the excitation signal and C is the capacitance[20,21] when the exponent P is equal to 1 (a condition well satisfied in the present case). The whole equivalent circuit and the fitted response (solid points) are shown in Figs. 5a and b, respectively.

The physical–chemical meaning of the R-CPE terms is assessed in the following way. The typical width of space within the measured system where the given relaxation process occurs is estimated from the formula for the capacitance of a parallel plate capacitor:

$$w=\frac{\varepsilon\varepsilon_0 A}{C} \tag{3}$$

where ε is the relative dielectric constant of the medium, ε_0 is the permittivity of a vacuum, A is the surface area of the electrodes and C is the measured capacity. The estimated relative dielectric constant of the present materials, regardless of the precise composition, is of the order of 100. Using the three values of C pertaining to the three CPE elements (see Fig. 5) gives the following typical widths within the present pellets: (a) the width

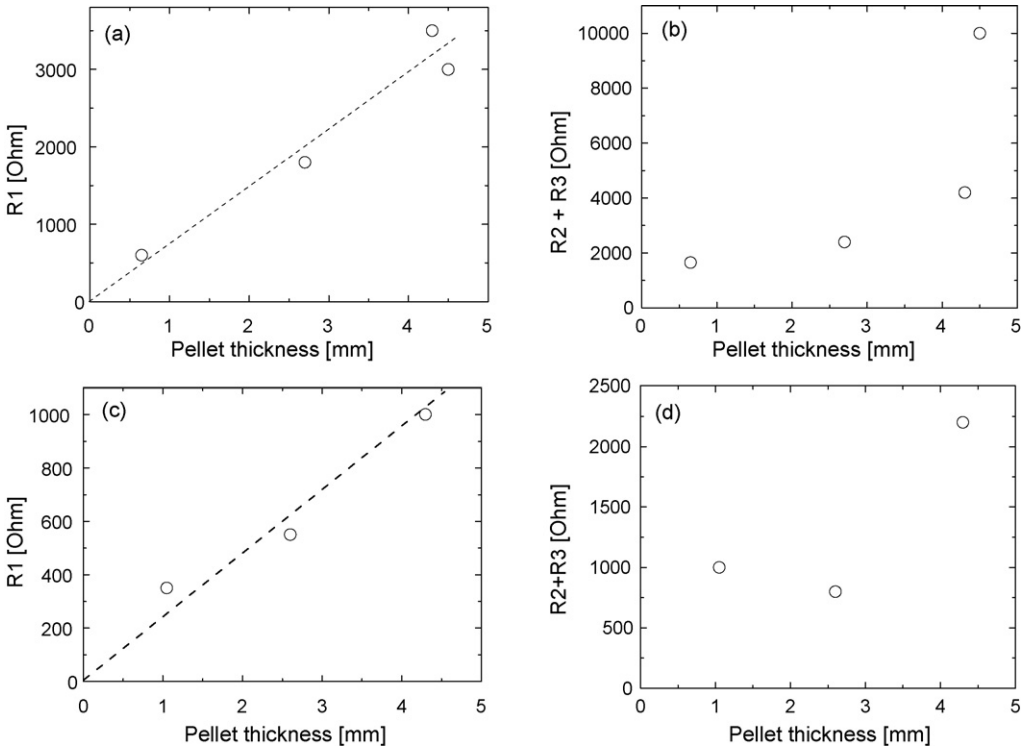

Fig. 6. Resistances determined on the basis of the equivalent circuit in Fig. 5 as functions of the pellet thickness. Graphs (a) and (b) correspond to a series of samples with composition $x = 0.1$, graphs (c) and (d) correspond to another series of samples with $x = 0.4$. R1 is the resistance of the arc appearing at high frequencies, R2 + R3 is the total resistance of the arc appearing at low frequencies (i.e., the right arc in Fig. 5).

corresponding to the high-frequency process is about 11 μm, (b) the two processes observed in the low-frequency arc have similar typical widths: 120–240 nm. The latter values are in the order of magnitude that corresponds to the two space-charge regions created between the pellet and the two gold contacts. The calculated space-charge widths should then correspond to the so-called Debye length of the space-charge region:

$$w_D = L_D \equiv \sqrt{\frac{\varepsilon\varepsilon_0 k_B T}{e^2 c_0}} \quad (4)$$

where k_B is Boltzmann's constant, T is the temperature, e is the charge of the carrier forming the space-charge region and c_0 is the bulk concentration of that carrier.

Based on Eqs. (3) and (4) and the known dielectric constant ($\varepsilon = 100$), we find that at room T the concentration of charge carrier(s) that constitute(s) the space charge is about 2.5×10^{15}–1×10^{16} cm^{-3}. We will assume that this same type determines the total conductivity of our samples.

Based on the well-established models of ceramic materials,[22,23] we expect that at higher frequencies the bulk grain and/or grain-boundary response due to the present polycrystalline sample will be observed. As mentioned above, the fit at the highest frequencies is already good enough if only one R-CPE term is used (see also Fig. 5). This means that, in fact, either the bulk grain or the grain-boundary response strongly prevails. From the calculated width (Eq. (3)) associated with this response (11 μm), we immediately realize that it cannot be due to the bulk response because the actual thickness of the pellet measured in Fig. 5 was about 245 times higher (about 2.7 mm). This leads us automatically to a conclusion that at high frequencies we must observe the response of the grain boundaries between the two electrodes, while the bulk grain response should be negligibly small. In other words, the grain-boundary conductivity is much smaller than that of the grain and thus prevails in the high-frequency response.

In order to further verify the proposed conduction model, we performed another independent test: we measured the impedance spectra of pellets with different thicknesses. To avoid spurious effects, and to allow for some generalization, two parallel series of samples with different compositions were measured. We fitted all the measured spectra with the equivalent circuit shown in Fig. 5b. The low- and high-frequency resistances as functions of the pellet thickness are shown in Fig. 6. We can see that for both parallels the high-frequency resistance is proportional to the pellet thickness (Fig. 6a and c). This confirms that the high-frequency response is due only to the inherent properties of the pellet. The magnitude of the low-frequency arc (the sum of both low-frequency resistances), however, does not show any systematic dependence on the pellet's thickness. This is expected because the contact resistance between the deposited metal and the underlying pellet is a highly sensitive quantity depending on the sputtering conditions, the handling, etc.

In the next experiments we checked to see if in the present temperature range (25–300 °C) oxygen vacancies could play any role in the conduction mechanism. First, we found that the oxygen partial pressure had no influence on the grain-boundary conductivity (Fig. 7). This could indicate that up to 300 °C the

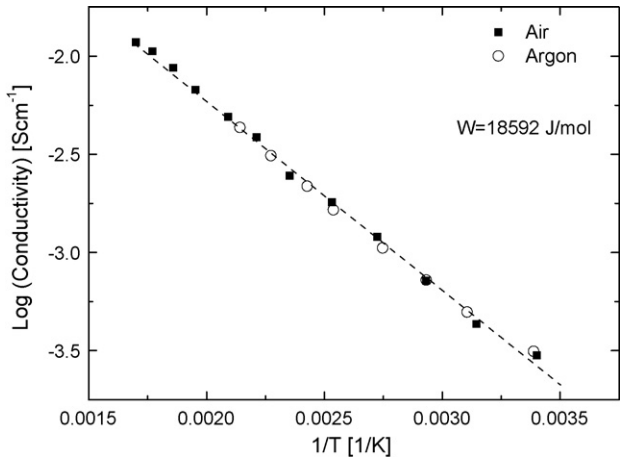

Fig. 7. Influence of atmosphere (air, argon) on the Arrhenius plot for the high-frequency conductivity (calculated from R1 and the pellet dimensions). To avoid possible effects due to pre-heating in a given atmosphere, different pellets (prepared from the same batch) were used for each of the measurements. The dashed line serves as a guide for the eye only.

oxygen defects are either present in a very small concentration or are frozen in position. The role of these vacancies will be further discussed in the next section.

Fig. 8 shows that the Arrhenius activation energy is more or less independent of composition in the range from $0.1 \leq x \leq 0.45$ and has a value of 0.175 ± 0.005 eV. This implies that within this compositional range the conduction mechanism probably remains the same. It is unusual, however, that the isothermal conductivity as a function of composition (see the two selected conductivity isotherms in Fig. 9) reaches a maximum at a given composition. Namely, it is difficult to imagine a scenario where either the concentration of defects and/or their mobility would reach a maximum at a certain composition, if the conduction mechanism remains unchanged. We tried to find an alternative explanation for this unusual phenomenon. In particular, we noticed that the average grain sizes of samples having a different composition varied quite significantly. Indeed, as shown in Table 1, the average grain size has a maximum exactly at the composition $x = 0.25$, where the conductivity maximum is also observed (cf. Fig. 9). Of course, a bigger grain size means a smaller number of grain boundaries between the electrodes and thus a lower resistance (higher conductance). To be sure of this effect, we additionally prepared samples with the same composition but with different average grain sizes (we achieved these with different sintering times). As expected, and in agreement with our conduction model introduced above, the conductivity was roughly proportional to the average grain size (not shown).

Despite the considerable grain-size effect on the conductivity, we must emphasize that the variation in grain size alone cannot explain the variation of the conductivity in Figs. 8 and 9. For example, going from $x = 0.1$ to $x = 0.04$, the conductivity drops by more than an order of magnitude (see Fig. 8a), while the grain size is not decreased significantly. To explain this additional, non-geometrical effect, we check and discuss several possible mechanisms of point-defect formation in the present system.

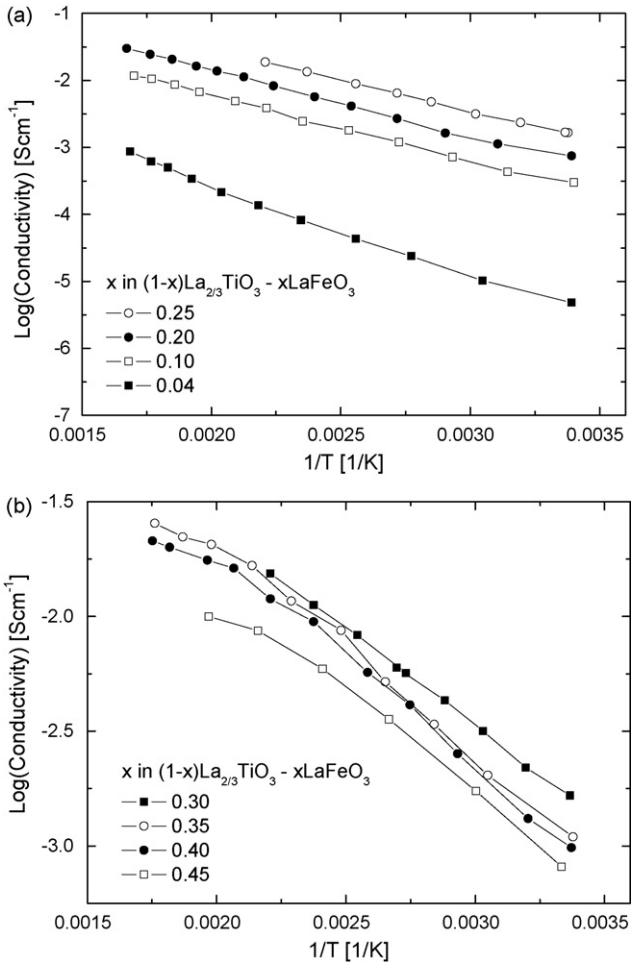

Fig. 8. Arrhenius plots for pellets having different compositions.

3.4. Possible mechanisms explaining the occurrence of point defects in $La_{2/3}TiO_3$–$LaFeO_3$

There are various possible scenarios that could explain the occurrence of point defects in the present system. First, we note that the major defects are most likely $(V_{La})^x$, $(Ti_{Ti})'$, $(Fe_{Ti})''$, $(Fe_{Ti})'$, $(Fe_{Ti})^x$ and $(V_O)^{\bullet\bullet}$ (in this paper the Kröger-Vink notation is used). By contrast, in the perovskite structure interstitial ions cannot be present as major defects. As indicated already in Introduction, our previous investigation of the electrical conductivity of a $La_{2/3}TiO_3$ compound stabilized with 4 mol% $LaAlO_3$ showed that the ceramic behaved as an electrical insulator with a high resistivity ($>10^{12}$ Ω cm), suggesting that the vacancies on the La sites (V_{La}) were not ionized at room temperature.[19] Based on these data, four possible sources for the conductive species related to the formation mechanisms of the $La_{2/3}TiO_3$–$LaFeO_3$ solid solution can be proposed:

(i) The formation of an intimate composition of two perovskites, $La_{2/3}TiO_3$ and $LaFeO_3$, on the unit-cell level, as described by Eq. (1). It may be concluded that all ions and A-site vacancies are neutral, similar to the case of the $La_{2/3}TiO_3$–$LaAlO_3$ system.[19] Such a system, however,

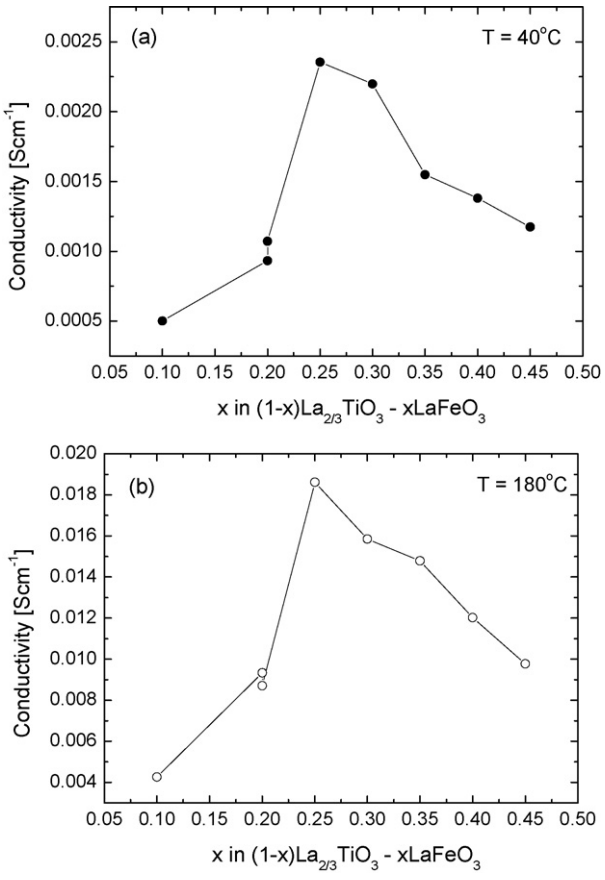

Fig. 9. Conductivity as a function of pellet composition at (a) 40 °C and (b) 180 °C.

behaves as an electrical insulator due to the absence of conducting species.

(ii) It is known that at high sintering temperatures, the reduction of Fe^{3+} to Fe^{2+} (which could be a source of free electrons) is more likely than the reduction of Ti^{4+} and Ti^{3+}.[24] However, a Mössbauer phase analysis excluded the presence of Fe^{2+} ions in our ceramic samples fired in an air atmosphere.[25]

(iii) Based on the remaining probable defects, i.e., $(Fe_{Ti})^x$, $(Fe_{Ti})'$ and $(V_O)^{\bullet\bullet}$, the following reaction can be proposed: Fe occupies, as a Fe^{3+} ion, the Ti site in the perovskite structure, whereupon a corresponding number of oxygen vacancies are created:

$$1/2Fe_2O_3 + 1/3La_2O_3 \rightarrow 2/3(La_{La})^x + (Fe_{Ti})' + 5/2(O_O)^x + 1/2(V_O)^{\bullet\bullet} \quad (5)$$

A similar reaction mechanism was also reported by Warren et al.[26] when explaining the incorporation of Fe in the $BaTiO_3$ structure. They assumed that the Fe ions that substitute for Ti^{4+} ions on the B-sites keep the 3+ valence. In this case, Fe^{3+}–$V_O^{\bullet\bullet}$ complexes appear in the ceramics. Generally, the $V_O^{\bullet\bullet}$ is considered to be the most mobile intrinsic ionic defect in oxide perovskite ceramics. However, as shown by the present experiments (Fig. 7), at least in the low-temperature region, the role of oxygen vacancies in the overall conduction mechanism is negligible.

Table 1
Typical size ranges and average grain sizes of selected $(1-x)$ $La_{2/3}TiO_3$–x $LaFeO_3$ samples

Composition (x)	Size range (minimum–maximum size) (μm)	Estimated average size
0.10	50–150	100
0.20	10–100	50–60
0.25	50–1000	350
0.30	50–500	100–150
0.35	10–120	50
0.40	200–300 in matrix: 2–5	

(iv) Alternatively, a certain amount of iron on the Fe_{Ti} sites in the $(La_{(2+x)/3}V_{(1-x)/3})(Ti_{(1-x)}Fe_x)O_3$ solid solution may be ionized to Fe^{4+} ions, thus creating a corresponding number of free electrons:

$$(Fe_{Ti})' \rightarrow (Fe_{Ti})^x + n' \quad (6)$$

Reaction (6) could explain the rapid increase in the conductivity from $x = 0.04$ (where the number of generated electrons is still negligible) to $x = 0.1$. Above $x = 0.1$, the increase in conductivity should be proportional to the increase in x, if Eq. (6) was the only mechanism affecting the conductivity. However, as pointed out above, no such linearity is observed because at different compositions, different average grain sizes are formed (see Table 1). Based on our results and methods it is not possible to "deconvolute" the total conductivity into its individual contributions. A method that could be useful for this purpose is micro-contact impedance spectroscopy, where the conductance of grains and grain boundaries can be probed separately.[27,28]

4. Conclusion

$LaFeO_3$ stabilizes the$La_{2/3}TiO_3$ perovskite structure *via* the same mechanism as previously observed with $LaAlO_3$,[4] that is, *via* formation of a solid solution with a general formula $(1-x)La_{2/3}TiO_3$–$xLaFeO_3$. The solid solution forms in the wide range of $0.04 \leq x \leq 1$. We propose that Fe incorporates into the Ti sites homogeneously and that the number of vacancies at the La sites decreases with increasing Fe content. The crystal structure of the solid solution transforms from orthorhombic to tetragonal at $x = 0.2$, becomes cubic in the range $0.3 < x < 0.8$, and transforms again into orthorhombic (typical for pure $LaFeO_3$) above that range.

The conductivity of prepared solid solutions exceeds that of pure $LaFeO_3$ (1.5×10^{-6} S cm^{-1})[9,10] by several orders of magnitude—the highest room temperature value (1.7×10^{-3} S cm^{-1}) has been obtained at $x = 0.25$. The conductivity across grain boundaries is much less than across the bulk grains so bigger grains will, as a rule, give higher average conductivities.

It has been found that at low temperatures (up to 300 °C) the conduction mechanism does not involve the movement of oxygen vacancies. Among the several possible electron-conduction mechanisms, the one involving ionization of the Fe_{Ti} sites into Fe^{4+} ions and electrons seems the most plausible; it explains the

rapid increase in the conductivity from $x = 0.04$ (where the number of generated electrons is still negligible) to $x = 0.1$. Above $x = 0.1$, the further changes in conductivity are a result of interplay between this mechanism and the fact that the conductivity is very much affected by the average grain size.

The very high electronic conductivity of the present $(1-x)La_{2/3}TiO_3$–xLaFeO3 perovskite-based solid solution holds promise for achieving a good mixed conductivity at high temperatures. If so, it would be worth checking the potential applicability of this material as a cathode material for solid oxide fuel cells.[29,30]

Acknowledgement

Financial support from the Slovenian Research Agency is fully acknowledged.

References

1. Abe, M. and Uchino, K., X-ray study of the deficient perovskite $La_{2/3}TiO_3$. *Mater. Res. Bull.*, 1974, **9**, 147–156.
2. MacChesney, J. B. and Sauer, H. A., The system La_2O_3–TiO_2. *J. Am. Ceram. Soc.*, 1962, **45**(9), 416–422.
3. Škapin, S. D., Kolar, D. and Suvorov, D., Phase stability and equilibria in the La_2O_3–TiO_2 system. *J. Eur. Ceram. Soc.*, 2000, **20**, 1179–1185.
4. Škapin, S. D., Kolar, D. and Suvorov, D., X-ray diffraction and microstructural investigation of the Al_2O_3–La_2O_3–TiO_2 system. *J. Am. Ceram. Soc.*, 1993, **76**(9), 2359–2362.
5. Tien, T. Y. and Hummel, F. A., Solid solutions in the system $SrTiO_3$–(La_2O_3:3TiO_2). *Trans. Br. Ceram. Soc.*, 1967, **66**(5), 233–245.
6. Sasaki, H. and Matsuo, Y., Oxidation–reduction phenomena in the $PbTiO_3$–$La_{2/3}TiO_3$ system. *Ceram. Bull.*, 1972, **51**(2), 164–166.
7. Belous, A. G., Gavrilova, L. G., Polinecka, S. V., Makarova, Z. R. and Chaljich, V. P., Stabilizacia perovskitnog strukturnji titanata lantana. *Ukr. Khim. Zh.*, 1984, **50**(5), 460–461.
8. Suvorov, D., Valant, M., Škapin, S. D. and Kolar, D., Microwave dielectric properties of ceramics with compositions along the $La_{2/3}TiO_{3(STAB)}$–$LaAlO_3$ tie-line. *J. Mater. Sci.*, 1998, **33**, 85–89.
9. Subba Rao, G. V., Wanklin, B. M. and Rao, C. N. R., Electrical transport in rare earth *ortho*-chromites, -manganites and -ferrites. *J. Phys. Chem. Solids*, 1971, **32**, 345–358.
10. Kuščer, D., Hrovat, M., Holc, J., Bernik, S. and Kolar, D., Some characteristics of Al_2O_3- and CaO -modified $LaFeO_3$-based cathode materials for solid oxide fuel cells. *J. Power Sources*, 1996, **61**, 161–165.
11. Mizusaki, J., Yoshihiro, M., Yamauchi, S. and Fueki, K., Nonstoichiometry and defect structure of the perovskite-type oxides $La_{1-x}Sr_xFeO_{3-\delta}$. *J. Solid State Chem.*, 1985, **58**, 257–266.
12. Grilli, M. L., Di Bartolomeo, E. and Traversa, E., Electochemical NO_x sensors based on interfacing nanosized $LaFeO_3$ perovskite-type oxide and ionic conductors. *J. Electrochem. Soc.*, 2001, **148**(9), H98–H102.
13. Waernhus, I., Vullum, P. E., Holmestad, R., Grande, T. and Wiik, K., Electronic properties of polycrystalline $LaFeO_3$. Part I. Experimental results and the qualitative role of Schottky defects. *Solid State Ionics*, 2005, **176**, 2783–2790.
14. Marezio, M. and Dernier, P. D., The bond lengths in $LaFeO_3$. *Mater. Res. Bull.*, 1971, **6**, 23–30.
15. Goodenough, J. B., *Metalic Oxides in Progress in Solid State Chemistry, Vol 5*. Pergamon, Oxford, 1971, pp. 149–399.
16. Hole, I., Tybell, T., Grepstad, J. K., Waernhus, I., Grande, T. and Wiik, K., High temperature transport kinetics in heteroepitaxial $LaFeO_3$ thin films. *Solid-State Electron.*, 2003, **47**, 2279–2282.
17. Mizusaki, J., Sasamoto, T., Cannon, W. R. and Bowen, H. K., Electronic conductivity, Seebeck coefficient, and defect structure of $LaFeO_3$. *J. Am. Ceram. Soc.*, 1982, **65**(8), 363–368.
18. Kolar, D., Škapin, S. D., Suvorov, D. and Valant, M., Phase equilibria and dielectric properties in the La_2O_3 - Ga_2O_3 -TiO_2 system. In *SPEAR, Proceedings of the Ninth International Conference on High Temperature Materials Chemistry, Vol IX*, ed. E. Karl, 1997, pp. 109–115 (*Proceedings Vol* 97–39), Pennington: The Electrochemical Society.
19. Škapin, S., Phases and properties of ceramics based on BaO–TiO_2–La_2O_3–Al_2O_3 system, PhD Thesis, Faculty for Natural Sciences and Technology, Ljubljana, Slovenia, 1997.
20. Raistrick, D., Macdonald, J. R. and Franceschetti, D. R., In *Impedance Spectroscopy Emphasizing Solid Materials and Systems*, ed. J. R. Macdonald. J. Wiley & Sons, New York, 1987, pp. 27–132.
21. Kerner, Z. and Pajkossy, T., On the origin of capacitance dispersion of rough electrodes. *Electrochim. Acta*, 2000, **46**, 207–211.
22. Bauerle, J. E., Study of solid electrolyte polarization by a complex admittance method. *J. Phys. Chem. Solids*, 1969, **30**, 2657–2670.
23. Bonanos, N., Steel, B. C. H., Butler, E. P. *et al.*, In *Impedance Spectroscopy Emphasizing Solid Materials and Systems*, ed. J. R. Macdonald. J. Wiley & Sons, New York, 1987, pp. 191–238.
24. Desu, S. B. and Subbarao, E. C., Inhibition of reduction of $BaTiO_3$. *J. Mater. Sci.*, 1980, **15**, 2113–2115.
25. Hanžel, D., Hanžel, D., Meisel, W. and Kraševec, V., Mössbauer and TEM studies of the perovskite system $(1-y)La_{2/3}\square_{1/3}TiO_3$·$y$LaFeO$_3$. *Hyperfine Interact.*, 1994, **92**, 1019–1025.
26. Warren, W. L., Vanheusden, K., Dimos, D., Pike, G. E. and Tuttle, B. A., Oxygen vacancy motion in perovskite oxides. *J. Am. Ceram. Soc.*, 1996, **79**(2), 536–538.
27. Škapin, A. S., Pejovnik, S. and Jamnik, J., Determination of the local electrical properties in ceramic materials gained by microcontact impedance spectroscopy. *J. Eur. Ceram. Soc.*, 2001, **21**, 1759–1762.
28. Škapin, A. S., Gaberščček, M., Dominko, R., Bele, M., Drofenik, J. and Jamnik, J., Detection of highly conductive pathways in $LiMn_2O_4$-carbon black composites for Li ion batteries by microcontact impedance spectroscopy. *Solid State Ionics*, 2004, **167**, 229–235.
29. Kojima, T., Nomura, K., Miyazaki, Y. and Tanimoto, K., Synthesis of various $LaMO_3$ perovskites in molten carbonates. *J. Am. Ceram. Soc.*, 2006, **89**, 3610–3616.
30. Zhou, X.-D., Yang, J. B., Thomsen, E.-C., Cai, Q., Scarfino, B. J., Nie, Z. *et al.*, Electrical, thermoelectric, and structural properties of La(M_xFe_{1-x})O_3 (M = Mn, Ni, Cu). *J. Electrochem. Soc.*, 2006, **153**, J133–J138.